

Pressure effects on the diffusion and solubility of Zn in Pb†

D. L. Decker, R. A. Ross,* W. E. Evenson, and H. B. Vanfleet

Department of Physics and Astronomy, Brigham Young University, Provo, Utah 86402

(Received 20 September 1976)

We have measured the activation volume of Zn in Pb to be 3.98 ± 0.11 cm³/mole at 600 K and atmospheric pressure and have measured the temperature and pressure dependence of the saturation solubility of Zn in Pb. From the solubility measurements we find a volume of solution of 3.1 ± 0.3 cm³/mole, which is not consistent with purely interstitial or purely substitutional solution. These results are compared to other impurity diffusion in Pb.

INTRODUCTION

There has been much interest recently in attempting to determine the mechanism by which the noble metals diffuse in Pb. These, and the metals grouped on either side of them in the periodic table, have been found to diffuse in Pb from one to five orders of magnitude more rapidly¹⁻⁸ than Pb self-diffusion.⁹⁻¹¹ It has been recognized for some time that the large diffusivities and small activation energies for these metals cannot be explained in terms of a vacancy diffusion mechanism. The measurements of Miller^{4,12} on the enhancement of Pb self-diffusion by Au, Ag, and Cd additions lend support to this conclusion. His results showed more enhancement than would be expected for an interstitial mechanism, but not nearly enough for a vacancy mechanism.

Originally, attempts to explain differences in diffusivities and to pin down diffusion mechanisms were based primarily on comparison of activation energies. Kidson² used such arguments and proposed a dissociative mechanism for the diffusion of Au in Pb, similar to that suggested by Frank and Turnbull¹³ for Cu diffusion in Ge. Kidson assumed that Au dissolves both substitutionally and interstitially in Pb, with the majority of the Au atoms dissolving substitutionally. However, he assumed that the Au atoms at interstitial sites diffuse so much more rapidly than those at substitutional sites that the primary contribution to diffusion results from the former. Miller¹⁴ expanded upon this model in an attempt to explain the diffusivity and enhancement effect for Cd in Pb. He added an additional defect to those assumed by Kidson; namely, bound interstitial-vacancy pair. He assumed that the concentration of Cd defects in interstitial sites and the concentration of Cd defects in bound pairs were very small compared to the total Cd impurity concentration. Decker *et al.*⁸ expanded this model to accommodate arbitrary fractions of atoms diffusing via these mechanisms and calculated the effects of pressure on this mod-

el of diffusion.

Diffusion studies at high pressures provide additional tests for models of diffusion. Nachtrieb, Resing, and Rice¹⁵ measured the effect of pressure on Pb self-diffusion to 8 kbars, Hudson and Hoffman¹⁶ to 40 kbar, and most recently Baker and Gilder¹⁷ to 10 kbars. These workers reported the activation volume of lead self-diffusion as 0.73 ± 0.02 molar volumes. Gold diffusion in Pb has been studied to 10 kbars by Ascoli *et al.*¹⁸ and by Weyland, Decker, and Vanfleet¹⁹ to 50 kbars. Diffusion has also been measured for Ag, Cu, Ni, and Pd in Pb to pressures of 50 kbars.^{6-8,20,21} Schmutz *et al.*²² have studied Cd diffusion in Pb to 42 kbars. Finally, this work reports studies of Zn diffusion in Pb to 52 kbars. Activation volumes for impurity diffusion range from about 0.04 molar volumes for Pd in Pb to about 0.5 molar volumes for Hg in Pb. This range of activation volumes indicates that these impurities either diffuse by different mechanisms or that they diffuse by a multiple mechanism allowing a wide range of activation energies and volumes.

Other interesting experiments have been performed to help determine modes of solution for various metallic impurities in Pb. Miller and Edelstein²³ have measured the effect of isotopic mass on the diffusion of Cd in Pb. Miller *et al.*²⁴ have also measured the isotope effect for the diffusion of Ag in Pb. The results of these experiments are not at present in complete harmony with an interstitial dominated mechanism for diffusion of these impurities in Pb. Turner and co-workers^{25,26} and Sagues and Nowick²⁷ have performed measurements of anelastic relaxation effects for Cu-, Au-, and Ag-doped Pb. Their results are in conflict and are thus inconclusive. Warburton and Turnbull²⁸ have suggested some possible explanations for the conflict, but these experiments need repeating. Warburton²⁹ measured a deenhancement in the diffusivity of Au in Pb (Au) alloys with increasing Au concentration. Warburton and Turnbull³⁰ interpreted this in terms

of two modes of solution, one involving pairs or larger clusters of Au atoms and the other involving single Au atoms in interstitial sites. Such clustering would imply a binding between the Au impurities, and the fraction dissolving in clusters would increase with concentration, thus dehanding the diffusivity. Similar dehanding was sought in Ag diffusion in Pb (Ag) alloys but was not observed.³¹ Cohen and Warburton³² interpreted the resistivity data of Rossolimo and Turnbull on Pb (Au) alloys as a manifestation of this same clustering. Finally Ray, Hahn, and Giessen³³ have observed changes in the superconducting transition temperature for Pb doped with varying amounts of Au and Ag. From their results they conclude that the di-substitutional mode of solution is likely for Au and Ag in Pb.

There is not much information on the solubility of many of these diffusers in lead,³⁴ but what little there is seems to show an inverse correlation between solubility and diffusivity. There has been no study of the effects of pressure on solubility prior to this work.

EXPERIMENTAL PROCEDURE

Sample preparation has been described previously.⁷ However, in order to fit in the hydrostatic high-pressure chamber the lead samples were only 3 mm in diameter and 3 mm long. Crystal growth, plating procedures, and counting techniques were the same as described previously.

As explained by Ross *et al.*⁷ it was necessary to keep anneal times short to avoid complete depletion of the surface layer of Zn-65 by oxidation. This depletion caused back diffusion near the surface and a "hump" resulted in the concentration profile. This was also found to be the case for the high-pressure anneals. Most of the samples were annealed for times between 2 and 14 min, but one sample annealed at 477 °C was held at the anneal temperature for only 46 sec to avoid this problem.

The high-pressure anneals took place inside a 400-ton ram capacity cubic press. The hydrostatic pressure chamber consisted of liquid petroleum ether (B.P. 100–115 °C) contained in a 6.4-mm diam. inconel-X tube with polyethylene stoppers inserted in both ends. The tube was inserted, along the main diagonal of a 2.45-cm pyrophyllite cube, as shown in Fig. 1. Chromel-alumel thermocouple leads were inserted through one cube corner and through one stopper. The thermocouple junction was embedded into the end of the cylindrical lead crystal opposite the plated surface, in order to insure correct temperature readings.

The sample was heated by passing a current through the inconel-X tube which was connected electrically to two opposite anvils of the press by

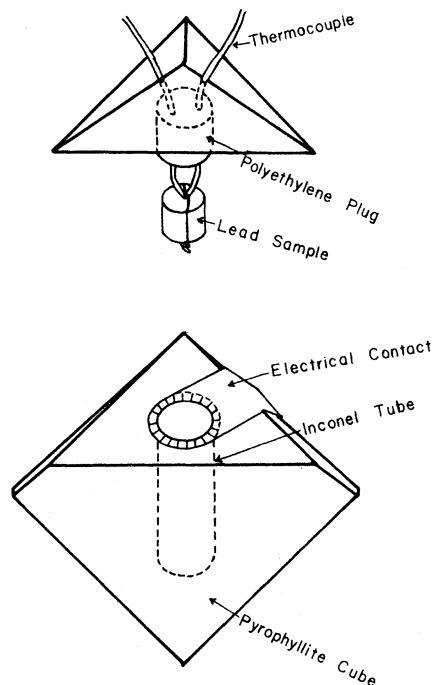


FIG. 1. High-pressure sample chamber. A 2.45-cm cube of pyrophyllite with an inconel tube, containing a fluid and the diffusion sample, passing diagonally through the cube.

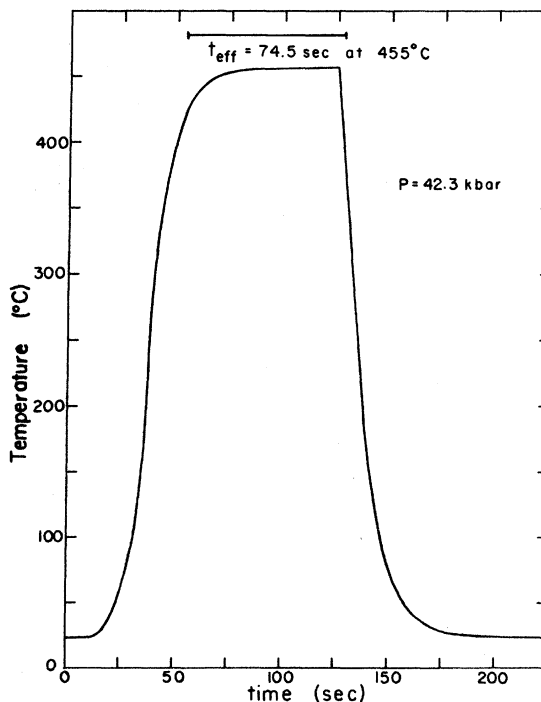


FIG. 2. Temperature-time profile for a short diffusion anneal at high pressure.

means of heating tabs also shown in Fig. 1. Temperatures were controlled by an electronic feedback device designed by Decker.³⁵ The necessarily short anneal times used for this experiment required improved response times, however, so the original design was modified by adding a 10-M Ω resistor to the feedback circuit in series with the capacitor; combined heating and cooling times totaled less than 50 sec using this method. The temperature-time profile for one very short diffusion run is shown in Fig. 2.

Pressure calibration was achieved by observing oil pressures at which the phase transitions of Hg, Bi, and Tl occurred at room temperature.³⁶ The effect of heating on the pressure inside the cell was determined by observing Bi phase transitions at various temperatures and pressures in a hydrostatic cell similar to the one used here.³⁷

METHOD OF ANALYSIS

Concentration profiles originally showed maximum impurity concentrations at penetration depths as great as 500 μm into the crystal, with lower concentrations just inside the plated surface. Reasons for these strange profiles have been discussed.⁷ However, when diffusion anneal times were shortened sufficiently, profiles resulted which fit the following solution to the one-dimensional diffusion equation

$$c = c_0 \operatorname{erfc}(x/(4Dt)^{1/2}), \quad (1)$$

where c is the impurity concentration, x is the penetration depth, t is the anneal time, D is the diffusion coefficient, and c_0 is the solubility of the impurity in the host for the given anneal temperature and pressure. This solution corresponds to the boundary condition of a constant concentration of impurity at $x=0$ during the entire anneal time. That Eq. (1) is the appropriate solution for short anneal times and low impurity solubility has been argued by Kidson.²

In addition to the experimental circumvention of this oxidation problem, we calculated the shape of the humped concentration profiles,³⁸ assuming a diffusion equation of the form

$$\partial c / \partial t = D(\partial^2 c / \partial x^2) - Wc\delta(x), \quad (2)$$

where D is the usual diffusivity and W is taken to be constant. The term $Wc\delta(x)$ represents a removal at the surface (by oxidation or other chemical reaction) of impurity atoms available to diffuse. The solution of this equation for initial condition $c(x, 0) = m\delta(x)$ is

$$c(x, t) = \frac{me^{-x^2/4Dt}}{(4\pi Dt)^{1/2}} \times \left[1 - W \left(\frac{\pi t}{4D} \right)^{1/2} e^{(Wt+x)^2/4Dt} \operatorname{erfc} \left(\frac{Wt+x}{(4Dt)^{1/2}} \right) \right]. \quad (3)$$

When we fit the concentration profile data to this equation, by a nonlinear least-squares routine, we find that the humped profiles are well represented by Eq. (3). The values of D obtained by this procedure also agreed, within experimental error, with the values of D obtained from shortening the diffusion time to remove the hump.

Experimental concentration profiles for all successful anneals were analyzed to find the best values for c_0 and the product Dt by a nonlinear least-squares fit to Eq. (1). Temperature versus time profiles were analyzed to correct anneal times for heating and cooling. These profiles were examined to give an initial estimate of an effective anneal time at temperature T and thus a diffusivity at each anneal temperature. Then using an estimated $D(T)$ we integrated over the temperature-time profile to improve the estimated anneal time and obtain new values of $D(T)$. This procedure was iterated to self-consistency. The final values of D for various temperatures and pressures could then be fit by least-squares analysis to an equation of the form

$$D = D_0 \exp[-(\Delta H + P\Delta V)/RT + (\text{second-order terms})], \quad (4)$$

where ΔH is the activation energy, ΔV is the activation volume, T is the absolute temperature, P is the pressure, and R is the gas constant. Details of the analysis are given by Weyland, Decker, and Vanfleet.¹⁹ The second-order terms involve the derivatives of the activation volume with respect to temperature and pressure, and the specific heat of activation ΔC_P . The variable parameters used in the least-squares analysis are D_0 , ΔH , ΔV , $(\partial \Delta V / \partial T)_P$, and $(\partial \Delta V, \partial P)_T$, with ΔC_P being related to the other derivatives as discussed by Gilder and Lazarus.³⁹

Without knowing the absolute efficiency of the counting system a relative saturation solubility as a function of pressure and temperature is measured directly from the tracer activity per unit volume and unit time extrapolated to the surface. One can interpret this data using the following thermodynamic argument.⁴⁰ Assume solid Zn metal is in equilibrium with a solid solution of Zn in Pb at pressure P and temperature T with Gibbs free energies per mole of Zn represented by G_s and $G_2 = G_2^0 + RT \ln a_2$, respectively. The

superscript "o" represents a reference state and the activity $a_2 = P_2/P_2^o$, because at these temperatures the vapor pressure of Zn is low enough to use an ideal-gas approximation. P_2 and P_2^o are the partial pressures of Zn above the alloy at (P, T) and of Zn in the alloy reference state, respectively. We define the reference state using Henry's law; $P_2 = \gamma x_2$, where γ is a constant and x_2 is the mole fraction of Zn in the Pb-Zn alloy. This law is correct in the limit of small x_2 , and we choose the nonphysical reference state to be the extension of Henry's law to $x_2 = 1$ so that $P_2^o = \gamma$. At equilibrium, where $x_2 = c_0$, the saturation solubility, and $G_s = G_2$:

$$G_2^o - G_s = \Delta G_s = -RT \ln c_0. \quad (5)$$

Expanding ΔG_s about $P = 0$, with $\Delta G_s(0) = \Delta H_s(0) - T\Delta S_s$ and $\partial \Delta G_s / \partial P = \Delta V_s = V_2^o - V_{Zn}$ we get

$$\ln c_0(P) = \Delta S_s / R - [\Delta H_s(0) + P\Delta V_s] / RT. \quad (6)$$

$V_2^o = V_2$ is the volume of a mole of Zn as a dilute impurity in metallic Pb and V_{Zn} is the volume of one mole of pure Zn metal. The measured results should have the pressure and temperature dependence explicitly shown in Eq. (6).

RESULTS

Forty-six anneals were made for which experimental errors were considered to be minimal. Pressures ranged from atmospheric pressure to 49 kbars and temperatures ranged from 180 to 500 °C. A typical concentration profile is shown in Fig. 3. The solid line is a least-squares fit of the data to Eq. (1).

Diffusion coefficients ranged from 8×10^{-7} to 1×10^{-8} cm²/sec. The experimental data are shown plotted along isobars in Fig. 4. Anneals were made at fixed values of ram load which thus corresponded to slightly different sample pressures due to temperature corrections. Therefore, some of the experimental D values had to be corrected in order to plot them on isobars. This correction was in all cases less than 1.8 kbars. The isobars were computed from the least-squares fit of the data to Eq. (4). Thus the slopes of the lines are essentially equal to $-(\Delta H/R + P\Delta V/R)$. The measured values of D were typically accurate to $\pm 5\%$ with some points with very short anneals being somewhat more uncertain.

The results of the analysis of the diffusion of Zn in Pb are summarized in Table I. The activation energy for Zn diffusion in Pb was found to increase from 11.4 ± 0.2 kcal/mole at zero pressure to 17.7 ± 0.4 kcal/mole at 48 kbars. The activation volume increased from 0.21 molar volumes at zero pressure to 0.24 molar volumes at 48 kbars

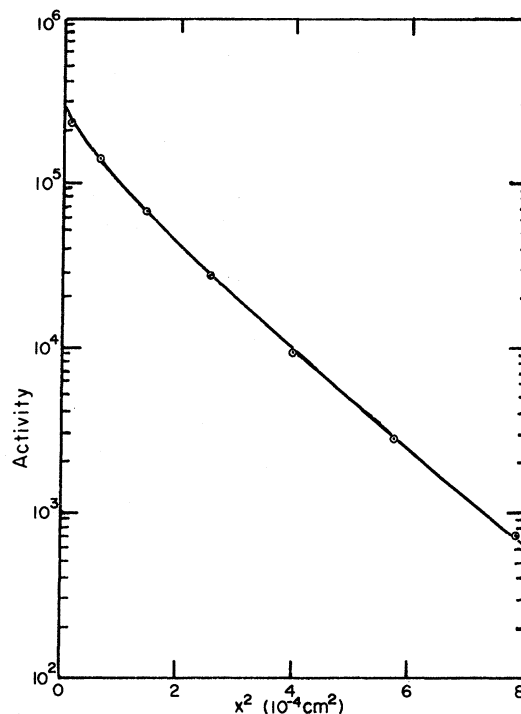


FIG. 3. Penetration profile of ⁶⁵Zn after being diffused into Pb at 31.7 kbars, 435 °C for 60 sec. The line is the best fit to Eq.(1).

(evaluated at 600 K). For a given pressure, the activation volume is nearly independent of temperature decreasing from 0.224 ± 0.007 molar volumes at 180 °C to 0.212 ± 0.006 at the melting point at atmospheric pressure. This change is not outside the error bars.

Solid solubility data for Zn in Pb were reported previously⁷ at atmospheric pressure. Relative solubility data are shown in Fig. 5 for three isobars as a function of reciprocal temperature. These data were fitted by least-squares methods to Eq. (6) to yield the enthalpy of solution, $\Delta H_s(0) = 10.62$ kcal/mole and the volume of solution, $V_2 - V_{Zn} = 3.1 \pm 0.3$ cm³/mole = $(0.169 \pm 0.005)V_0$. The lines in Fig. 5 show the least-squares fit.

The eutectic temperature probably increases with pressure although it is not clear how to detect this temperature from diffusion measurements. If the eutectic composition is not altered by pressure then the difference between the eutectic and the melting temperature versus pressure will remain nearly constant and the eutectic will be at the point *E* in Fig. 5 on the 21.4-kbar line. This would indicate a strong increase of the saturation solubility at the eutectic with pressure. We did not make diffusion measurements nearer the melting temperature because of the short times required to avoid surface reaction of the Zn.⁷

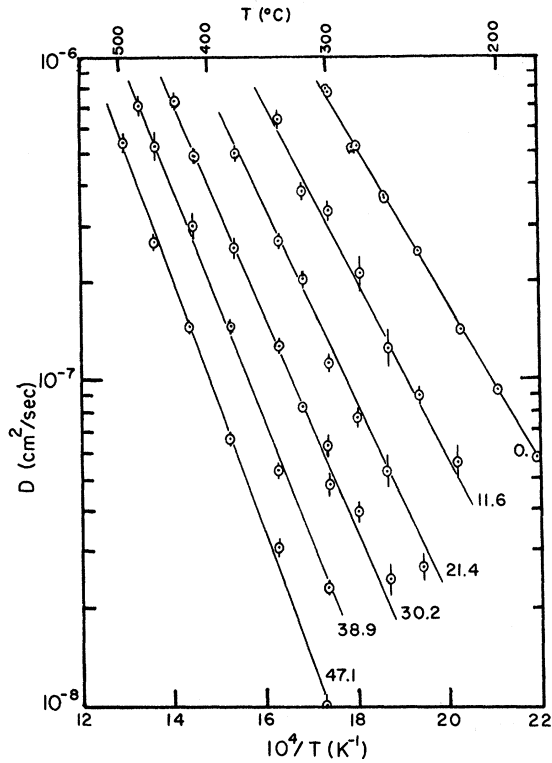


FIG. 4. Arrhenius plots of the diffusion of Zn in Pb along selected isobars with the pressure of each isobar given in kbar. The lines are a least-squares fit to Eq. (4).

DISCUSSION AND CONCLUSIONS

The diffusion of Zn in Pb has not been measured before. There are no measurements of the isotope effect or linear enhancement effects on this diffusion and little else is known about Zn impurities in Pb. Since these results cannot be correlated with other measured properties of Zn in Pb, we will compare the Zn diffusion results with those of other defects in lead. We have recently published a paper⁸ in which the pressure effects on diffusion of eight different impurities in Pb were simultaneously collated into a defect theory as-

TABLE I. Diffusion parameters for zinc in lead at atmospheric pressure and 600 K.

$D_0(\text{cm}^2/\text{sec})$	0.0165 ± 0.0026
$\Delta H(\text{kcal/mole})$	11.42 ± 0.16
$\Delta V/V_0$	0.212 ± 0.006
$\partial(\Delta V/V_0)/\partial P(10^{-3} \text{ kbar}^{-1})$	1.20 ± 0.24
$\partial(\Delta V/V_0)/\partial T(10^{-4}/\text{K})$	-0.86 ± 0.28
$\Delta C_p/R$	-0.63 ± 0.24

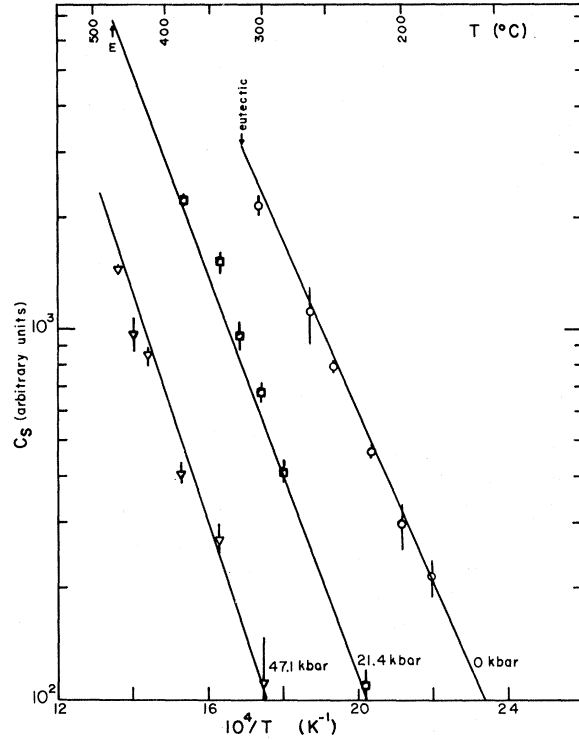


FIG. 5. Saturation solubility vs reciprocal temperature along selected isobars. The eutectic at atmospheric pressure is indicated and also the expected eutectic (E) at 21.4 kbars. The lines are from a least-squares fit to Eq. (6).

suming an equilibrium distribution of substitutional, interstitial, and bound interstitial-vacancy ($i-v$) pair defect states. The assumptions of the theory were rather severe, but the conclusions may serve as a guide to further analysis of defect states and diffusivities in lead. The results for Zn diffusion in Pb indicate that 80% of the observed diffusivity at 600 K results from motion of free Zn interstitial atoms, albeit only 10% of the Zn impurities are in interstitial sites. The remainder of this diffusion comes from the motion of Zn atoms in interstitial positions bound to a lattice vacancy; about 45% of the Zn atoms are in this type of defect state at 600 K, with the remaining 45% of the Zn atoms being substitutional in the Pb. Certain energy terms were also predicted such as 0.09 eV for the energy to form an ($i-v$) pair from a substitutional Zn atom and 0.51-eV binding energy of an interstitial and a vacancy. This analysis also indicates that when an atom changes from a substitutional to an interstitial site the crystal volume increases by $\Delta V_{is} \equiv V_i - V_s = (0.110 \pm 0.005)V_0$ and $\Delta V_{ps} \equiv V_p - V_s = (0.57 \pm 0.03)V_0$,

where V_p is the formation volume of an $(i-v)$ pair. Combining these results with the volume of solution reported here, $V_{sol} = qV_i + pV_p + sV_s - V_{Zn} = (0.169 \pm 0.005)V_0$ yields $V_s = (0.40 \pm 0.04)V_0$, which predicts a larger Pb relaxation into a substitutional site containing a Zn atom than for an empty substitutional site (vacancy). This might mean an effective attraction between Zn and Pb atoms and could be the cause of the formation of $(i-v)$ pairs. Such a pair could be formed simply by the tendency for the Zn to move away from the substitutional site toward a neighboring Pb atom if such an attractive interaction exists. From the symmetry of the fcc crystal one would expect the $(i-v)$ pair to form a defect with a $[100]$ oriented tetragonal strain in the lattice and should show an anelastic relaxation peak.

At present the various theoretical models have too many variables to relate them directly to the limited information on the diffusion of Zn in Pb; however, there are some interesting observations that one can make relative to the experimentally measured activation volume. If we plot the activation volume versus the doubly ionized atomic radius for each impurity in Pb, we find a strong correlation (Fig. 6). This is especially surprising since little correlation is evident if the abscissa is chosen as r^+ , r^{3+} , or the covalent radius, etc. We do not know what this dependence means because the atomic radius is not a well-defined physical quantity. Does this indicate that these defects have an effective valence of 2 in Pb? As is shown in Fig. 6 the point for Pb self-diffusion does not lie on the line formed by the impurities diffusing in Pb. Perhaps *all* these other elements diffuse by

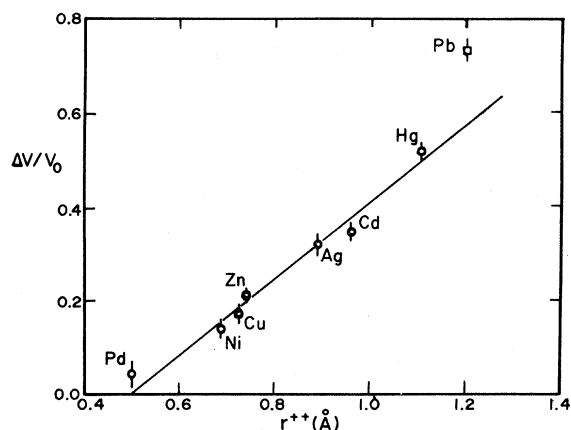


FIG. 6. Graph of the activation volume versus the doubly-ionized atomic radius (from Ref. 42).

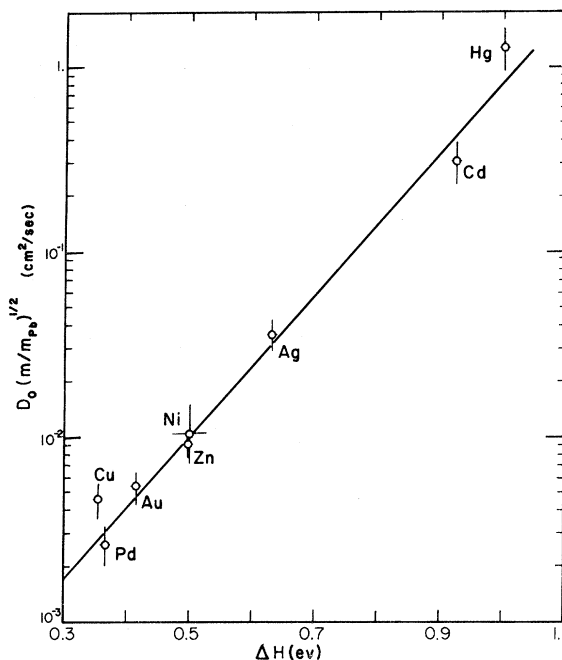


FIG. 7. $\text{Log}[D_0(m/m_{\text{Pb}})^{1/2}]$ vs activation energy for several elements diffusing in Pb.

the same basic mechanism but one which is different from that of lead self-diffusion.

Zener⁴¹ derives an expression for D_0 for chemical diffusion which is particularly simple for several elements all diffusing in the same host. He gives

$$D_0 = \gamma a^2 \nu e^{\lambda(\beta \Delta H / kT_m)}, \quad (7)$$

where $\gamma = 1$ for a fcc lattice, a is the lattice parameter, ν is the vibrational frequency which we will take as $\nu_0(m/m_{\text{Pb}})^{1/2}$, where m is the atomic mass and ν refers to the vibrational frequency of a Pb atom. ΔH is the activation energy, T_m the melting temperature, λ is a numerical coefficient less than one, but of the order of unity, and $\beta = -d(\mu/\mu_0)/d(T/T_m)$ where μ refers to an appropriate elastic modulus. Zener estimated $\beta = 0.5$ for Pb. We rewrite (7) as follows:

$$\ln D_0(m/m_{\text{Pb}})^{1/2} = \ln a^2 \nu_0 + (\lambda\beta/kT_m)\Delta H. \quad (8)$$

So we should find a linear relation between $\ln D_0(m/m_{\text{Pb}})^{1/2}$ and ΔH . The results for all defects diffusing in Pb are shown in Fig. 7. The least-squares linear fit gives $\lambda\beta = 0.47$ from the slope and $\nu_0 = 5 \times 10^{10} \text{ sec}^{-1}$ from the intercept. Not only do we observe a linear relation, but the parameters are reasonably close to one's physical expectations although ν_0 appears to be rather small.

†Work supported in part by the NSF.

*Present address: IBM Corp., San Jose, Calif.

¹A. Ascoli, *J. Inst. Met.* **89**, 218 (1961).

²G. V. Kidson, *Philos. Mag.* **13**, 247 (1966).

³B. F. Dyson, T. Anthony, and D. Turnbull, *J. Appl. Phys.* **37**, 2370 (1966).

⁴J. W. Miller, *Phys. Rev.* **181**, 1095 (1969).

⁵W. K. Warburton, *Phys. Rev. B* **7**, 1330 (1972).

⁶C. T. Candland and H. B. Vanfleet, *Phys. Rev. B* **7**, 575 (1973).

⁷R. A. Ross, H. B. Vanfleet, and D. L. Decker, *Phys. Rev. B* **9**, 4026 (1974).

⁸D. L. Decker, C. T. Candland, and H. B. Vanfleet, *Phys. Rev. B* **11**, 4885 (1975).

⁹B. Okkerse, *Acta Metall.* **2**, 551 (1954).

¹⁰N. H. Nachtrieb and G. S. Handler, *J. Chem. Phys.* **23**, 1969 (1955).

¹¹H. A. Resing and N. H. Nachtrieb, *J. Phys. Chem. Solids* **21**, 40 (1961).

¹²J. W. Miller, *Phys. Rev. B* **2**, 1624 (1970).

¹³F. C. Frank and D. Turnbull, *Phys. Rev.* **104**, 617 (1956).

¹⁴J. W. Miller, *Phys. Rev.* **188**, 1074 (1969).

¹⁵N. H. Nachtrieb, H. A. Resing, and S. A. Rice, *J. Chem. Phys.* **31**, 135 (1959).

¹⁶J. B. Hudson and R. E. Hoffman, *Trans. Metall. Soc. AIME (Am. Inst. Min. Metall. Pet. Eng.)* **221**, 761 (1961).

¹⁷A. G. Baker and H. M. Gilder, *Bull. Am. Phys. Soc.* **20**, 442 (1975).

¹⁸A. Ascoli, B. Bollani, G. Guarini, and D. Kustudic, *Phys. Rev.* **141**, 732 (1966).

¹⁹J. A. Weyland, D. L. Decker, and H. B. Vanfleet, *Phys. Rev. B* **12**, 4225 (1971).

²⁰H. R. Curtin, D. L. Decker, and H. B. Vanfleet, *Phys. Rev.* **139**, A1552 (1965).

²¹D. L. Decker, *Phys. Rev. B* **11**, 1770 (1975).

²²J. D. Schmutz, H. B. Vanfleet, D. L. Decker, and W. E. Evenson, *Bull. Am. Phys. Soc.* **19**, 672 (1974).

²³J. W. Miller and W. A. Edelstein, *Phys. Rev.* **188**,

1081 (1969).

²⁴J. W. Miller, H. N. Mundy, L. C. Robinson, and R. E. Loess, *Phys. Rev. B* **8**, 2411 (1973).

²⁵T. J. Turner, S. Painter, and C. H. Nielsen, *Solid State Commun.* **11**, 577 (1972).

²⁶T. J. Turner and C. H. Nielsen, *Solid State Commun.* **15**, 243 (1974).

²⁷A. A. Sagues and A. S. Nowick, *Solid State Commun.* **15**, 239 (1974).

²⁸W. K. Warburton and D. Turnbull, *Thin Solid Films* **25**, 71 (1975).

²⁹W. K. Warburton, *Phys. Rev. B* **11**, 4945 (1975).

³⁰W. K. Warburton and D. Turnbull, in *Diffusion in Solids*, edited by A. S. Nowick and J. J. Burton (Academic, New York, 1975).

³¹A. N. Rossolimo and D. Turnbull, *Acta Metall.* **21**, 21 (1973).

³²B. M. Cohen and W. K. Warburton, *Phys. Rev. B* **12**, 5682 (1975).

³³R. Ray, S. H. Hahn and G. C. Giessen, *Acta Metall.* **20**, 1335 (1972).

³⁴M. Hansen, *Constitution of Binary Alloys* (McGraw-Hill, New York, 1958).

³⁵D. L. Decker, *Rev. Sci. Instrum.* **39**, 602 (1968).

³⁶D. L. Decker, W. A. Bassett, L. Merrill, H. T. Hall, J. D. Barnett, *Phys. and Chem. Ref. Data* **1**, 773 (1972).

³⁷D. L. Decker, J. D. Jorgensen, and R. W. Young, *High Temp.-High Press.* **7**, 331 (1975).

³⁸W. E. Evenson and D. L. Decker, *Bull. Am. Phys. Soc.* **19**, 346 (1974).

³⁹H. M. Gilder and D. Lazarus, *Phys. Rev. B* **11**, 4916 (1975).

⁴⁰J. R. Goates and J. B. Ott, *Chemical Thermodynamics* (Harcourt Brace Jovanovich, New York, 1971), Sec. 3.2.

⁴¹C. Zener, *J. Appl. Phys.* **22**, 372 (1951).

⁴²Taken from the Table of Periodic Properties of the Elements published by E. H. Sargent, 1964.